Synthesis of the Water Dispersible L-Valine Capped ZnS:Mn Nanocrystal and the Crystal Structure of the Precursor Complex: [Zn(Val)$_2$(H$_2$O)]

Cheong-Soo Hwang,* Narae Lee, Young-Ah Kim, and Youn Bong Park†

Department of Chemistry, Dankook University, Institute of Nanosensor and Biotechnology, Seoul 140-714, Korea
**E-mail: cshwang@dankook.ac.kr*
†Department of Chemistry, Chungnam National University, Daejeon 305-764, Korea
Received August 10, 2006

The L-Valinate anion coordinating zinc complex, [Zn(val)$_2$(H$_2$O)], was isolated and structurally characterized by single crystal X-ray crystallography. The crystal possess orthorhombic symmetry with a space group $P2_12_12_1$, $Z = 4$, and $a = 7.4279(2)$ Å, $b = 9.4342(2)$ Å, $c = 20.5862(7)$ Å respectively. The compound features a penta-coordinate zinc ion in which the two valine anion molecules are directly coordinating the central zinc metal ion *via* their N (amine) and O (carboxylate) atoms, and an additional coordination to zinc is made by water molecule (solvent) to form a distorted square pyramidal structure. In addition, further synthesis of the valine capped ZnS:Mn nanocrystal from the reaction of [Zn(val)$_2$(H$_2$O)] precursor with Na$_2$S and 1.95 weight % of Mn^{2+} dopant is described. Obtained valine capped nanocrystal was water dispersible and was optically characterized by UV-vis and solution PL spectroscopy. The solution PL spectrum for the valine capped ZnS:Mn nanocrystal showed an excitation peak at 280 nm and a very narrow emission peak at 558 nm respectively. The measured and calculated PL efficiency of the nanocrystal in water was 15.8%. The obtained powders were characterized by XRD, HR-TEM, and EDXS analyses. The particle size of the nanocrystal was also measured *via* a TEM image. The measured average particle size was 3.3 nm.

Key Words : Crystal structure of zinc valinate complex, ZnS:Mn nanocrystal, Water dispersible nanocrystal, Amino acid capping ligand, Single molecular precursor

Introduction

Semiconductor nano-sized and quantum confined materials have gained considerable interest during the past decade.[1-3] These materials offer unique technological applications for various photo electronic devices or even for advanced bio-technologies due to their size dependant physical and optical properties.[4-6] Recently developed manganese doped nano-crystallite ZnS:Mn[7] is of special interest due to its high photoluminescence efficiency and stability at ambient temperature, which are critical properties required for electro-luminescence devices. In addition, water dispersible semiconductor nanocrystals were developed and mainly used for the biosensor materials since they were expected to be much more efficient, sensitive, and stable than the commercial organic dyes used for the same purpose.[8-10] However, unfortunately those semiconductor nanocrystals are usually hydrophobic and hard to be introduced in a biological system. Therefore, to overcome this problem, one has to change the surface of the nanocrystals from hydrophobic to hydrophilic by capping with polar or charged molecules such as mercaptoacetic acid (MAA),[11,12] amino-acid,[13] or bis(2-ethylhexyl)sulfosuccinate (AOT).[14] Then the target biomolecules can be attached to the surface modified nanocrystals *via* covalent bonding or self assembly in the same phase. The manganese doped ZnS nanocrystal was considered as an ideal candidate material for a fluorescence biolabeling agent due to its long luminescence life time.[9] Further more, a single molecular precursor such as [Zn(S$_2$CNEt$_2$)$_2$] was shown to be very useful for the formation of pure ZnS based nano materials.[15] In this paper, the synthesis and optical characterization of the water dispersible valine capped ZnS:Mn nanocrystal and the crystal structure of the [Zn(Val)$_2$(H$_2$O)] complex, which is a useful precursor for the ZnS:Mn nanocrystal formation, are described.

Experimental

All the solvents except deionized water were purchased from Aldrich (reagent grade) and distilled prior to use. The starting materials including L-valine, ZnSO$_4$, MnSO$_4$, and Na$_2$S were purchased from Aldrich and used as received. The UV-vis absorption spectrum was recorded on a Perkin Elmer Lamda 25 spectrophotometer equipped with a deuterium/tungsten lamp. The FT-IR spectrum was recorded on a Perkin Elmer Spectrum One spectrophotometer (KBr Cell, Nujol). The solution photoluminescence spectrum was taken in a Perkin Elmer LS-45 spectrophotometer equipped with a 500 W Xenon lamp, 0.275 m triple grating mono-chrometer, and PHV 400 photomultiplitor tube. The PL efficiencies for the valine capped ZnS:Mn was calculated by comparing to the recommended standard material in liter-ature,[16] 0.1 M solution of Quinine sulfate in H$_2$SO$_4$ (Fluka) whose emission wave length and reported absolute quantum yield are 550 nm and 0.546 (22 °C) respectively. The NMR spectrum was obtained by Unity Inova 500NB (500 MHz, Varian) spectrometer, and the elemental analysis was per-

formed by EA 1000 (C/H/N/S Analyzer, CE instrument, Italy) elemental analyzer using dynamic flash combustion method. The powder XRD pattern diagram was obtained by using Rigaku 300 X-ray diffractometer with Cu Kα(1.54 Å) wavelength light source. HR-TEM images were taken with a JEOL JEM 3011 electron microscope with a MAG mode of 50 to 1500000, and the accelerating voltage was 40-120 kV. The samples for the TEM were prepared *via* dispersion into hexane solvent and placement on a carbon-coated copper grid (300 Mesh) followed by drying under vacuum. In addition, the elemental composition of the nanocrystal was determined by an EDXS (Energy Dispersive X-ray Spectroscopy) spectrum which was obtained *via* an EDXS collecting unit equipped in the TEM, with a Si (Li) detector in IXRF 500 system.

X-ray Single-Crystal Structure Determination. Diffraction data were collected on a Siemens SMART CCD diffractometer equipped with a normal focus, 2 kW sealed tube X-ray source and graphite monochromated Mo Kα radiation (λ = 0.71073 Å) at 193(2) K. Data reduction and absorption correction was carried out with the programs SAINT[17] and SADABS[18] respectively. The structure was solved by direct methods and refined on F^2 by full-matrix least squares using SHELXTL[19] program suit. All hydrogen atoms were placed geometrically and refined in the riding mode of the carbon atoms of the valine molecule. The complete data collection parameters and details of the structure solution and refinement are given in Table 1. Crystallographic data for the structure reported here has been deposited with the Cambridge Crystallographic Data Centre (Deposition No. CCDC-275691). The data can be obtained free of charge *via http://www.ccdc.cam.ac.uk/perl/catreq/catreq.cgi* (or from the CCDC, 12 Union Road, Cambridge CB2 1EZ, UK; fax: +44 1223 336033; e-mail: *deposit@ccdc.cam.ac.uk*).

Table 1. Crystal data and structure refinement for [Zn(val)$_2$(H$_2$O)]

Identification code	Znvaline
Empirical formula	$C_{10}H_{22}N_2O_5Zn$
Formula weight	315.67
Temperature	295(2) K
Wavelength	0.71073 Å
Crystal system, space group	Orthorhombic, $P2_12_12_1$
Unit cell dimensions	a = 7.4279(2) Å, α = 90 deg. b = 9.4342(2) Å, β = 90 deg. c = 20.5862(7) Å, γ = 90 deg.
Volume	1442.60(7) Å^3
Z	4
Calculated density	1.453 Mg/m^3
Absorption coefficient	1.716 mm^{-1}
F(000)	664
Crystal size	0.25 × 0.15 × 0.12 mm
Theta range for data collection	1.98 to 28.36 deg.
Limiting indices	$-9 \le h \le 8$, $-12 \le k \le 9$, $-27 \le l \le 20$
Reflections collected / unique	8531 / 3442 [R(int) = 0.0374]
Absorption correction	Empirical
Max. and min. transmission	0.801 and 0.729
Refinement method	Full-matrix least-squares on F^2
Data / restraints / parameters	3442 / 0 / 247
Goodness-of-fit on F^2	1.003
Final R indices [I>2sigma(I)]	R1 = 0.0393, wR2 = 0.0818
R indices (all data)	R1 = 0.0564, wR2 = 0.0900
Absolute structure parameter	0.002(18)
Largest diff. peak and hole	0.377 and −0.368 e Å^{-3}

Synthesis of [Zn(Val)$_2$(H$_2$O)] Complex. A solution of $ZnSO_4 \cdot 5H_2O$ (2.88 g, 10 mmol) in 50 mL of water was slowly added to a 50 mL aqueous mixture solution containing L-Valine (2.34 g, 20 mmol) and NaOH (0.8 g, 20 mmol) at *ca.* 5 °C (ice-water bath). The solution was warmed up to ambient temperature after 1 hour stirring. The volume of the solution was reduced down to approximately 50 mL by boiling the mixture. Then the flask was placed in a temperature controlled oven at 80 °C. Keeping the flask 14 days resulted in obtaining colorless block crystals. Yield: 2.32 g (74%), Elemental analysis, found (calcd) (%) for $C_{10}H_{22}N_2O_5Zn$: C 38.65 (38.04): H 7.38 (7.02): N 8.80 (8.87), FT-IR ν (cm^{-1}): 3157 (s), 2966 (s), 1585 (s), 1396 (m), 1110 (m), 722 (m), ^{1}H NMR [δ (ppm), D$_2$O] 4.63 (D$_2$O); 3.25 (d, 1H, J = 5 Hz); 2.09 (septet, 1H, J = 10 Hz); 1.90 (br, NH); 0.76 (d, 6H, J = 15 Hz), ^{13}C NMR [δ (ppm), D$_2$O, fixed TMS at 0 ppm]; 180.18 [C2]; 59.53 [C4]; 29.73 [C6]; 15.97 [C7, C8].

Synthesis of Valine Capped ZnS:Mn Nanocrystal. Preparation procedures are similar to the method reported by Yi *et al.*[20] to synthesize Histidine capped ZnS;Mn nanocrystal. Isolated crystal of **[Zn(Val)$_2$(H$_2$O)]** (1.58 g, 5 mmol) was redissolved in 50 mL of 1 M Tris buffer (Aldrich) solution. In another flask, $MnSO_4 \cdot H_2O$ (0.02 g, 0.1 mmol) and Na_2S (0.4 g, 5 mmol) was dissolved in a 20 mL of 0.01 M HCl solution. Then the mixture was transferred to the flask containing Zn complex under vigorous stirring. The flask was sealed and incubated *ca.* 1 hour at ambient temperature. Addition of ethanol resulted in white precipitation at the bottom. The white solid was separated *via* centrifuge and decanting the supernatant. Then the solid was dried ca. 24 hours in a vacuum oven (40 °C). FT-IR ν (cm^{-1}): 2923 (s), 2853 (s), 1460 (s), 1376 (m), 722 (m), Uv-vis: 290-320 nm (br) (λ_{max} = 305 nm). Solution PL (water, 25 °C): excitation 280 nm; emission 558 nm (excitation wave length was fixed at 280 nm), Quantum Yield (calcd.): 15.8%, HR-TEM, avg. particle size: 3.3 nm.

Results and Discussion

The zinc ion containing amino acid complexes have long been interested in biomedical and pharmaceutical field.[21] In 1980, they were found to have insulin mimetic activities that made STZ-rats normalized their high blood glucose level. Such results made them potential drug candidates for Type II diabetes.[22] In our group, for instance, several vanadium and zinc ion containing organometallic, including some α-amino acids, complexes and their significant insulin enhancing activities were studied and reported in the literature.[23]

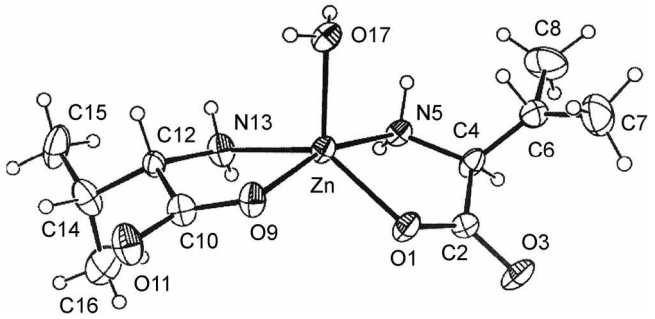

Figure 1. The ORTEP view of $[Zn(val)_2(H_2O)]$ including the atom numbering scheme. (30% ellipsoid probability); Selected bond lengths (Å) and angles (°): Zn-O(1) 2.017(2), Zn-O(9) 2.062(2), Zn-O(17) 2.034(3), Zn-N(5) 2.107(3), Zn-N(13) 2.077(4); O(1)-Zn-N(5) 80.83(10), O(9)-Zn-N(13) 80.67(11), O(1)-Zn-O(9) 86.66 (10), N(5)-Zn-N(13) 102.50(13), O(1)-Zn-O(17) 120.51(12), O(9)-Zn-O(17) 99.57(12), O(17)-Zn-N(5) 94.99(14), O(17)-Zn-N(13) 100.64(16), O(1)-Zn-N(13) 138.44(16), O(9)-Zn-N(5) 164.28(12).

The obtained crystal structure of $[Zn(val)_2(H_2O)]$ is illustrated in Figure 1. The crystal possess orthorhombic symmetry with the space group $P2_12_12_1$, $Z = 4$, with a = 7.4279(2) Å, b = 9.4342(2) Å, c = 20.5862(7) Å. The compound consists of two deprotonated valine molecules and a water molecule (solvent) coordinating directly to the zinc metal center. A characteristic feature of the structure is that central zinc ion has a penta-coordinate distorted square-planar geometry where the two valine molecules in the basal positions are coordinated to the metal *via* their N (amine) and O (carboxylate) atoms, and the fifth coordination in the apical position is by an oxygen atom in water (solvent) molecule. The bond distances between zinc and oxygen atoms in basal valine molecules are 2.062(2) Å and 2.017(2) Å respectively. The approximately 15° of distortion from the planar geometry in the basal $Zn(val)_2$ moiety is probably due to the two of the strained five membered ring structures made at the zinc center by the two valine molecules. The distance of Zn-O (water) in apical position, 2.034(3) Å, is slightly shorter than those for the basal positions.

The crystal structure of $[Zn(val)_2(H_2O)]$ can be compared to that of zinc-isovaline complex, $[Zn(iva)_2(H_2O)_2]_n$, reported by Strasdeit *et al.*[24] According to the authors, metal valinate and isovalinate complexes are among the most abundant amino acid containing compounds in meteorites which are believed to be a major source of amino acids in primitive earth. The structural difference between valine and isovaline is only made from the position of the methyl group. However, the crystal structure of the Zn-isovaline complex is quite different from that of our $[Zn(val)_2(H_2O)]$ complex. The compound can be synthesized from either ZnO or $ZnCl_2$. The crystal structure of $[Zn(iva)_2{\cdot}2H_2O]_n$ consists of a infinite chain structure made by carboxylate bridged $\{Zn(ival)_2\}$ moieties. In addition, unlike our compound, the two water solvent molecules are not directly coordinated to zinc metal center. The connected Zn-isovaline chains are also strongly connected to the upper and lower chains *via* hydrogen bonding between the isovaline molecules so that the whole 3D network polymeric structure is completed. Similar feature to the our $[Zn(val)_2(H_2O)]$ structure is that each zinc ion has penta-coordinate distorted square pyramidal geometry where the two isovaline molecules coordinate *via* their N (amine) and O (carboxylate) atoms, and the fifth coordination is from the oxygen atom in an isovaline belongs to the neighbor Zn-isovaline complex moiety. The bond distances between zinc and oxygen atoms in basal positions are 2.155(10) Å and 2.158(8) Å respectively, in which the average bond angle of O-Zn-N is approximately 86°. The distance of Zn-O (isovaline) in apical position, 2.123(5) Å, is slightly shorter than those for in the basal positions. In addition, there are several structures of valine containing mixed ligand complexes such as $[Zn_3Cl_2(val)_4]$[24] and Zinc valine with glycylglycinee-N-pyrimidine derivatives[25] reported in the literature. Those compounds contain similar penta-coordinate distorted square planar geometries at the zinc center with very similar bond distances of Zn-O (carboxylate) and Zn-N (amine) for the valine moiety to our $[Zn(val)_2(H_2O)]$ complex. The valine ligand in the complex was characterized by FT-IR spectroscopy, where the strong peaks at 2966, and 1585 cm^{-1} were assigned as zinc coordinated -NH_2 and -COO^- respectively.[26] However, the peak appeared at 2966 cm^{-1} was also possibly overlapped with that for C-H stretching band in the valine molecule.[27] In addition, a small portion of the crystal was dissolved in D_2O NMR solvent (Aldrich) to be characterized in the solution state. In ^{1}H-NMR spectrum, a broad peak appeared at 1.90 ppm was assigned as zinc coordinated NH, which was slightly up-field shifted from that for the free valine (2.00 ppm). In addition, in ^{13}C NMR spectrum all the carbon peaks appeared slightly up-field positions comparing to the free valine sample in the same solvent probably due to coordination to the electropositive zinc metal.

Water dispersible semiconductor nanocrystals were developed for fluorescent labeling technologies especially to be applied in biomedical area.[28] Unfortunately, most highly luminescent semiconductor nanocrystals are grown in hydrophobic media so that they are hardly compatible with biological systems. There are several reports of solubilized hydrophobic nanocrystals in water.[29-31] In those papers, the most commonly used synthetic scheme for the water dispersible nanocrystal is to use polar surface capping agents such as previously mentioned MAA and AOT molecules to form a micelle structure where the negative charges are distributed on the surface. In addition, it was shown that the photoluminescence efficiency for the AOT capped ZnS:Mn nanocrystal increased up to 7% after the surface modification.[29] This phenomenon resulted from the additional energy transfer of surfactant to Mn^{2+} metal ion as well as reducing the energy loss due to non-radioactive transition by the surface modification. Amino acids such as histidine[32] and cystein[33] were also developed as surface capping agents for ZnS non-doped nanocrystals. They were found to be very effective capping ligands in the synthesis of narrow range size distributed nanocrystals, which is difficult to achieve in aqueous solution due to different dissociation constants for

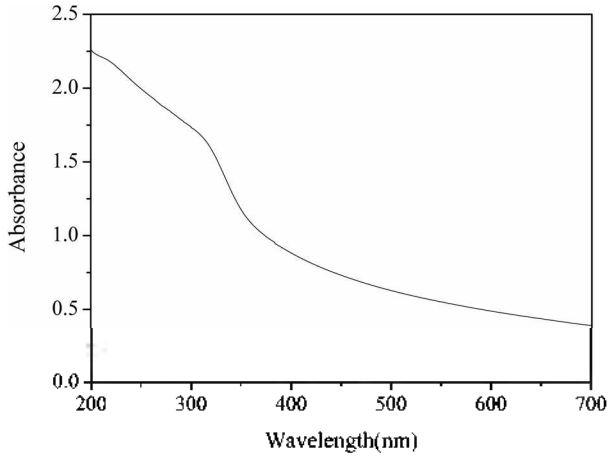

Figure 2. UV-vis absorption spectrum of the valine capped ZnS:Mn nanocrystal (water).

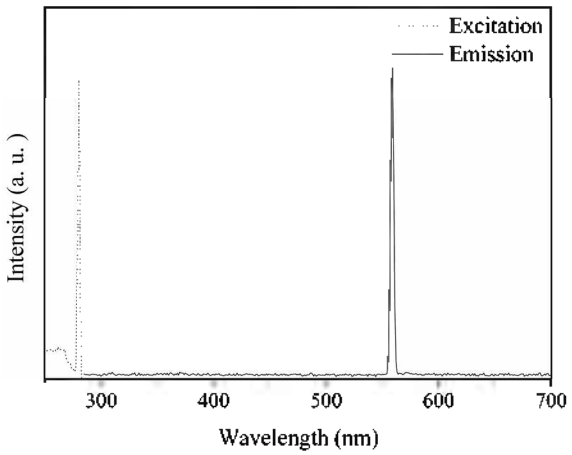

Figure 3. Solution PL spectrum of the valine capped ZnS:Mn nanocrystal (water). The emission spectrum was obtained by fixing the excitation wave length at 280 nm.

ZnS and MnS in water. Figure 2 shows a UV-vis absorption spectrum of the valine capped ZnS:Mn nanocrystal. A broad peak appeared from 290 to 320 nm and the maxima lies around 305 nm. Figure 3 presents the solution PL spectrum obtained from the valine capped ZnS:Mn in water, in which an excitation peak showed at 280 nm and a very narrow emission peak appeared at 558 nm respectively. The emission spectrum was obtained that the excitation wave length was fixed at 280 nm. In addition, the calculated PL efficiency was 15.8% compared to Quinine sulfate standard. These results are comparable for the previously reported histidine capped ZnS:Mn nanocrystal which showed excitation peak at 387 nm and the emission peak at 581 nm. More over, the calculated PL efficiency for the histidine capped ZnS:Mn nanocrystal was 18.0%, which is close to our valine capped ZnS:Mn nanocrystal.[34] The observed large stoke shift for the valine capped ZnS:Mn nanocrystal is one of the typical features appeared in nano-sized crystalline materials. For instance, a similar feature has been observed for the water soluble AOT capped CdS nanocrystal. The excitation peak appeared at 400 nm and the emission peak

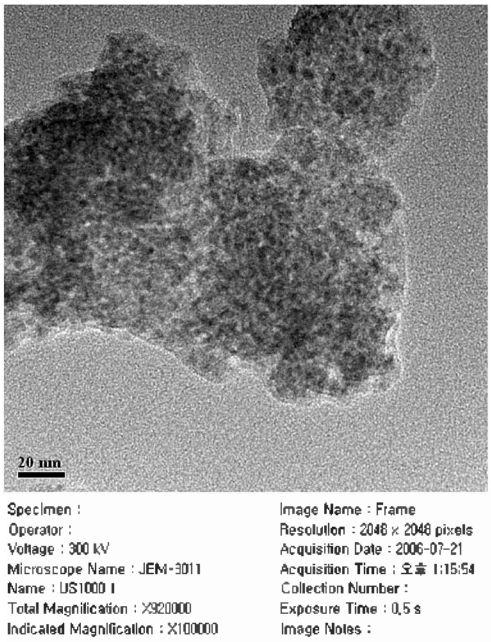

Figure 4. HR-TEM image of the valine capped ZnS:Mn nanocrystal, the scale bar represents 20 nm.

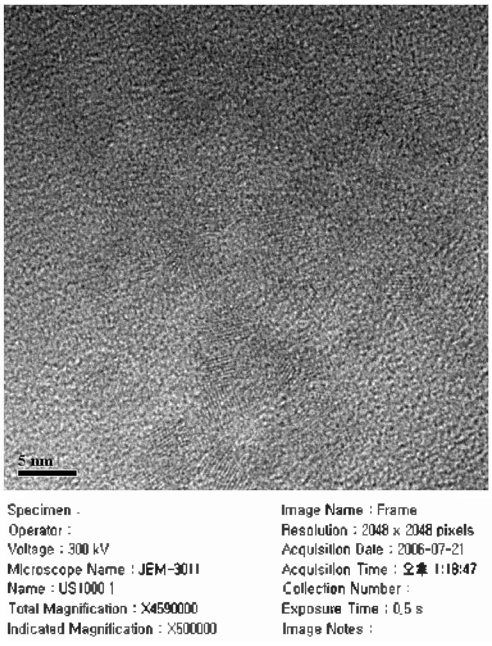

Figure 5. HR-TEM image of the valine capped ZnS:Mn nanocrystal, the scale bar represents 5 nm.

appeared at 540 nm, which showed a 140 nm stoke shift.[35] According to the authors, the phenomenon was due to the recombination of trapped charge carriers as opposed to free carriers. The trapping of the charge carriers occurs at surface defects that lie between the band gap states.

The particle sizes of the nanocrystals were measured *via* a HR-TEM image presented in Figure 4 and Figure 5. According to the pictures, the shapes of the particles are fairly homogeneous and the measured particle sizes are about 3.3 nm in average, which is marginally smaller than

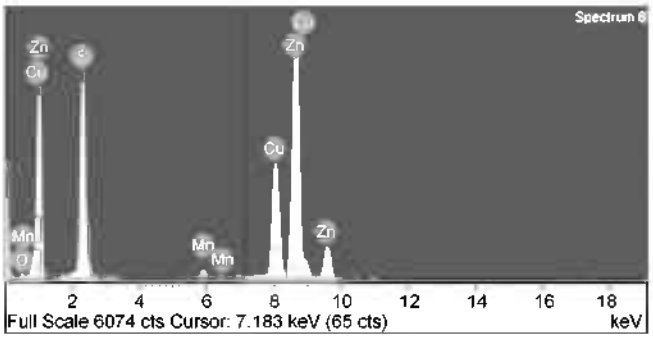

Figure 6. EDXS spectrum for the valine capped ZnS:Mn nanocrystal.

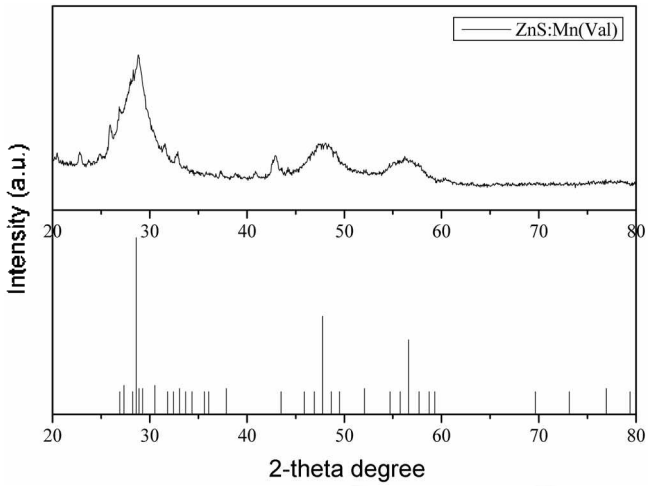

Figure 7. Powder XRD pattern diagrams of the valine capped ZnS:Mn nanocrystal (above) and bulk ZnS solid (below, cubic zinc blende).

that for the histidine capped ZnS:Mn nanocrystal (8.3 nm in average). In the figures a little agglomeration between the particles was observed due to the evaporation of the solvent during the sample preparation. However, the appearance of distinct lattice plane in the HR-TEM image (Fig. 5) with about 4 Å lattice spacing indicates that the product solids are single crystals rather than poly-crystalline aggregates. The EDXS spectrum was provided in Figure 6, which shows that the elemental compositions of the solid. The spectrum confirms the formation of the ZnS:Mn nanocrystal. In addition, the EDXS elemental analysis also indicated that the weight percent of the manganese among the measured particle was 1.95%, while those for zinc and sulfur were 69.73 % and 28.32 % respectively.

Figure 7 shows the wide angle X-ray diffraction patterns of a powder sample of the valine capped ZnS:Mn nanocrystal. In the diagram, appeared peaks were quite broad, which is quite common feature for nanosized crystalline materials; however, there were indexable peaks for (111), (220) and (311) planes, indicating that the nanocrystals are in a cubic zinc blende phase.[11] The surface capping valinate molecules were also characterized *via* FT-IR spectroscopy as the spectrum presented in Figure 8. To remove any uncoordinated valine or unreacted valinate complex, the

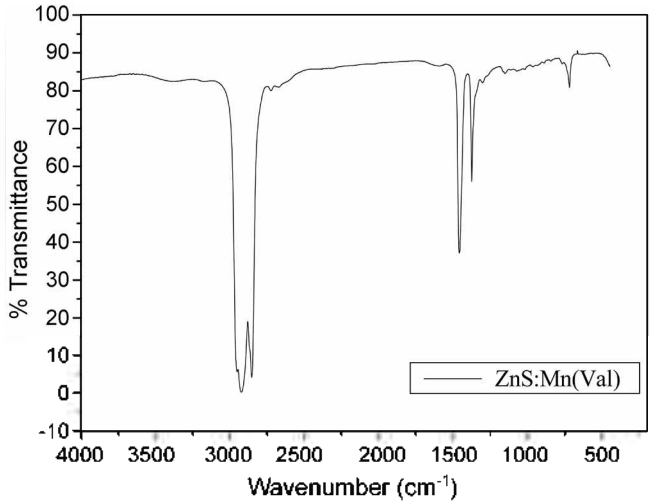

Figure 8. FT-IR spectrum of the valine capped ZnS:Mn nanocrystal (Nujol mull).

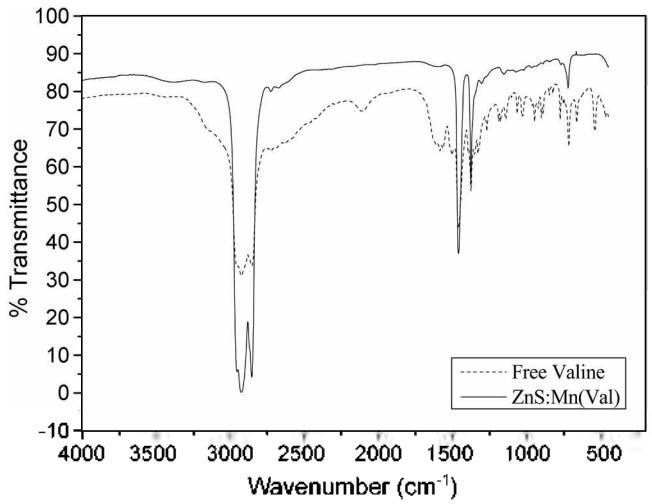

Figure 9. Overlapped FT-IR spectra of the valine capped ZnS:Mn nanocrystal (solid line) and the free valine molecule (dashed line).

centrifuged white solid was washed several times with cold alcohol/water mixture solutions rapidly. As a result, we were not able to find peaks corresponding free valine or zinc-valinate precursor complex in the IR spectrum, which is also demonstrated in Figure 9. In addition, the spectrum confirms that the valinate ligands are attached on the surface of the ZnS:Mn nanocrystal to provide a water dispersible nature for the originally hydrophobic ZnS:Mn nanocrystal.

Conclusion

The L-Valine, one of essential α-amino acids in human nutrition, coordinating zinc ion complex, $[Zn(val)_2(H_2O)]$, was isolated and structurally characterized by single crystal X-ray crystallography. The crystal possess orthorhombic symmetry with a space group $P2_12_12_1$, $Z = 4$, and a = 7.4279(2) Å, b = 9.4342(2) Å, c = 20.5862(7) Å respectively. The compound features a penta-coordinate zinc ion in which the two valine anion molecules are directly coordinating the

central zinc metal ion *via* their N (amine) and O (carboxylate) atoms, and an additional coordination to zinc is made by water molecule (solvent) to form a distorted square pyramidal structure. The second part of this work is about synthesis of the valine capped ZnS:Mn nanocrystal from the reaction of $[Zn(val)_2(H_2O)]$ precursor with Na_2S and 1.95 weight % of Mn^{2+} dopant. Obtained valine capped nanocrystal was water dispersible and was optically characterized by UV-vis and solution PL spectroscopy. The solution PL spectrum for the valine capped ZnS:Mn nanocrystal showed an excitation peak at 280 nm and a very narrow emission peak at 558 nm respectively. The measured and calculated PL efficiency of the nanocrystal in water was 15.8%. The particle size of the nanocrystal was also measured *via* a TEM image. The measured average particle size was 3.3 nm. One of the reasons that we synthesized the water-soluble ZnS:Mn semiconductor nanocrystal is to bind it to biomolecules, such as DNA and protein, so that they can be used as a biosensor material. In that point of view, the water soluble valine capped ZnS:Mn nanocrystal showed a sufficient PL efficiency to be applied to a microchip-scale biosensor system. Further bioconjugation study for the water soluble ZnS:Mn nanocrystal is progressing in our lab.

References

1. (a) Bol, A. A.; Meuijernk, A. *Phys. Rev. B* **1998**, *24*, 58. (b) Bruchez, M.; Morrone, M.; Gin, P.; Weiss, S.; Alivisatos, A. P. *Science* **1998**, *281*, 2013.
2. Alivisatos, A. P. *J. Phys. Chem.* **1996**, *100*, 13226.
3. Brus, L. E. *Appl. Phys. A* **1991**, *53*, 465.
4. Milliron, D. J.; Alivisatos, A. P.; Pitois, C.; Edder, C.; Frechet, J. M. *J. Adv. Mater.* **2003**, *15*, 58.
5. Jaiswal, J. K.; Mattoussi, H.; Mauro, J. M.; Simon, S. M. *Nature Biotechnol.* **2002**, *21*, 47.
6. Heath, J. R. *Acc. Chem. Res.* **1999**, 32.
7. Hwang, J. M.; Oh, M. O.; Kim, I.; Lee, J. K.; Ha, C.-S. *Curr. Appl. Phys.* **2005**, *5*, 31.
8. Mattousi, H.; Mauro, J. M.; Goldman, E. R.; Anderson, G. P.; Sundar, V. C.; Mikulec, F. V.; Bawendi, M. G. *J. Am. Chem. Soc.* **2000**, *122*, 12142.
9. Chan, W. C. W.; Nie, S. *Science* **1998**, *281*, 2016.
10. Alivisatos, A. P. *Science* **1996**, *271*, 933.
11. Zhuang, J.; Zhang, X.; Wang, G.; Li, D.; Yang, W.; Li, T. *J. Mater. Chem.* **2003**, *13*, 1853.
12. Hwang, C.-S.; Cho, I. H. *Bull. Kor. Chem. Soc.* **2005**, *26*(11), 1776.
13. Mirkin, C. A.; Letsinger, L. C.; Mucic, R. C.; Storhof, J. J. *Nature* **1996**, *382*, 607.
14. Kuobo, T.; Isobe, M.; Senna, M. *J. Lumin.* **2002**, *99*, 39.
15. Barrelet, C.; Wu, Y.; Bell, D. C.; Lieber, M. *J. Am. Chem. Soc.* **2003**, *125*, 11498.
16. Melhuish, W. H. *J. Phys. Chem.* **1961**, *65*, 229.
17. *SAINT: SAX Area-Detector Integration Program*, version 4.050; Siemens Analytical Instrumentation, Inc.: Madison, WI, 1995.
18. *SADABS: Area-Detector Absorption Correction*; Siemens Industrial Automation, Inc.: Madison, WI, 1996.
19. Siemens *SHELXTL, Structure Determination Software Programs*; Siemens Analytical X-ray Instruments Inc.: Madison, Wisconsin, USA, 1997.
20. Yi, G.; Sun, B.; Yang, F.; Chen, D. *J. Mater. Chem.* **2001**, *11*, 2928.
21. Chen, M. D.; Liou, S. J.; Lin, P. Y.; Yang, V. C.; Alexander, P. S.; Lin, W. H. *Biol. Trace. Elm. Res.* **1998**, *61*, 303.
22. Coulston, L.; Dandona, P. *Diabetes* **1980**, *29*, 665.
23. Seale, A. P.; de Jesus, L. A.; Kim, S. Y.; Choi, Y. H.; Lim, H. B.; Hwang, C.-S; Kim, Y. S. *Biothech. Lett.* **2005**, *27*, 221.
24. Strasdeit, H.; Busching, I.; Behrends, S.; Saak, W.; Berklage, W. *Chem. Eur. J.* **2001**, *7*(5), 1133.
25. Garzon, R. L.; Godino-Salido, M. L.; Arranz-Mascaros, P.; Fontecha-Camara, M. A.; Gutierrez-Valero, M. D.; Cuesta, R.; Moreno, J. M.; Stoekli-Evans, H. *Inorg. Chim. Acta* **2004**, *357*, 2007.
26. (a) Moszczenski, C. W.; Hooper, R. J. *Inorg. Chim. Acta* **1983**, *70*, 71 (b) Nakamoto, K. *Infrared and Raman Spectra of Inorganic and Coordination Compounds*, Part B, 5th ed.; Wiley: 1997; p 59.
27. Pandiarajan, S.; Umadevi, M.; Rajaran, R. K.; Ramakrishinan, V. *Spectrochim. Acta A* **2005**, *62*, 630.
28. (a) Chan, W. C. W.; Nie, S. *Science* **1998**, *281*, 2016. (b) Reiss, P.; Quemard, G.; Carayon, S.; Bleuse, J.; Chandezon, F.; Pron, A. *Mater. Chem. Phys.* **2004**, *84*, 10.
29. Gerion, D.; Pinaud, F.; Williams, S. C.; Parak, W. J.; Zanchet, D.; Weiss, S.; Alivisatos, A. P. *J. Phys. Chem. B* **2001**, *195*, 8861.
30. Chen, C. C.; Yet, C. P.; Wang, H. N.; Chao, C. Y. *Langmuir* **1999**, *15*, 6845.
31. Mitchell, G. P.; Mirkin, C. A.; Letsinger, R. L. *J. Am. Chem. Soc.* **1999**, *121*, 8122.
32. Kho, R.; Nguyen, L.; Torres-Martinez, C. L.; Mehra, R. K. *Biochem. Biophys. Res. Commun.* **2000**, *272*, 29.
33. Bae, W.; Mehra, R. K. *J. Inorg. Biochem.* **1998**, *70*, 125.
34. Bhargava, R. N.; Gallagher, D. *Phys. Rev. Lett.* **1994**, *72*, 416.
35. Tata, M.; Banerjee, S.; John, V. T.; Waguespack, Y.; Mcpherson, G. *Coll. Surf. A Phys. Chem. and Eng. Asp.* **1997**, *127*, 39.